

Fracture Toughness of WWER Uranium Dioxide Fuel Pellets with Various Grain Size

R. Sivov, V. Novikov, E. Mikheev, A. Fedotov

JSC "VNIINM", Moscow, Russian Federation

Introduction

Pelleted uranium dioxide is now used as a nuclear fuel for WWER. It is well known that, compared with metallic materials, ceramic materials have positive physical and chemical properties, viz., high melting temperature, hardness, durability, corrosion resistance, resistance to chemicals, and others. A drawback of ceramics, which limits their applications, is brittleness. As a measure of brittleness, the fracture toughness is an important characteristic of uranium dioxide fuel pellets.

The mechanical properties of pellets play an important role in the interaction of fuel and cladding. For linear power growth, the integrity of the cladding depends on the capacity of the fuel to balance the growing stress by means of plastic deformation and creep or by microcracking. The emission of gaseous fission products beneath the cladding via radial cracks is due to the prone of the fuel matrix to local cracking. Aside from in-reactor conditions during standard operation, these problems can become critical during non-standard reactor situations or transient regimes, since they can lead to accidents.

Analysis has shown [1–8] that one method of investigating the fracture toughness of ceramics, including based on uranium dioxide, is to make indentations, using a diamond tip, with cracks being formed on the of the samples. Compared with mechanical tests, this method of evaluating the mechanical properties of brittle materials is effective and inexpensive.

Uranium dioxide fuel pellets with grain sizes 13, 26, and 33 μm for WWER were investigated in the present work in order to determine crack formation and the fracture toughness.

1. Experimental

Crack formation was studied on three batches of WWER-type (batches P1, P2, and P3) uranium oxide fuel pellets, all manufactured commercially. Basic physical and chemical characteristics of pellets are presented in the Table 1. The content of impurity elements did not exceed the technical specifications.

Young's modulus (the elastic modulus) of the pellets was found at room temperature using the MUZA setup (Russia) and the ultrasonic resonance method, which consisted of exciting longitudinal ultrasonic waves in the sample and measuring its characteristic resonance frequency. The calculation was performed using the relation

$$E = 4h^2 f^2 k_f \rho, \quad (1)$$

where h is the height of the pellet, m; f is the characteristic resonance frequency of the oscillations, sec^{-1} ; k_f is the form factor, which depends on the height-to-diameter ratio of the sample; and ρ is the density of the pellet, kg/m^3 .

The microhardness was determined by the Vickers method with the maximum force applied to the sample equal to 1 kg. The Vickers microhardness test consists in making an imprint by indentation into the surface of the test sample under a static load applied for a definite period of time (usually 10–15 sec) to a diamond tip, which comprises a regular rectangular pyramid with apex angle 136° between the opposite faces (Fig. 1). The Vickers hardness is the ratio of the testing force to the surface area of the indentation found from the

Table 1. Basic physical and chemical characteristics of pellets

Characteristic	Batch		
	P1	P2	P3
Oxygen ratio (O/U)	2,0016	2,0024	2,0016
Density, g/cm^3	10,59	10,53	10,57
Average effective grain diameter, μm	13	26	33

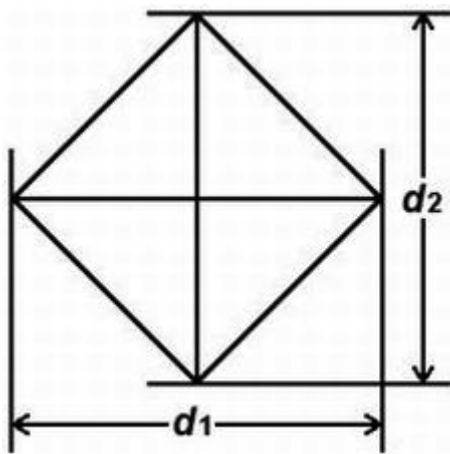


Figure 1. Imprint in the surface of the sample

average length of its diagonals:

$$H_V = \frac{2mg \sin \frac{\Theta}{2}}{d^2}, \quad (2)$$

where m is the load, kg; g is the acceleration of gravity; $\Theta = 136^\circ$; and d is the average length of two diagonals $(d_1 + d_2)/2$, m.

The fracture toughness is the resistance of the material to the advancement of a crack in it. In linear fracture mechanics, the stress intensity factor K is used to describe the stress field near the crack tip. The condition for the onset of crack propagation can be formulated as the stress reaching a critical value. Then, if K_1 is the stress intensity factor for the loading conditions under which the crack edges move in a direction normal to the plane of the crack (first mode of deformation), then K_{1c} is the critical stress intensity factor of the first mode of deformation under static loads, which determines the stress intensity with rapid propagation of a crack. The factor K_{1c} is called the fracture toughness.

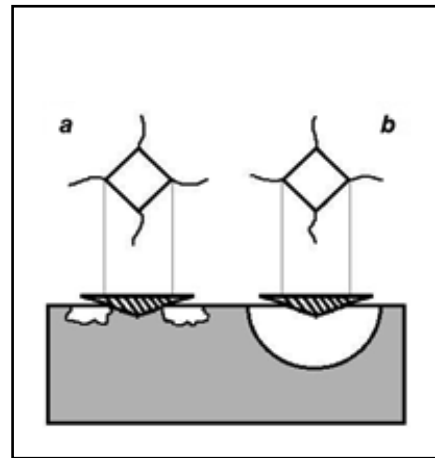


Figure 2. Palmqvist (a) and half-penny (b) cracks

A Mitutoyo HM-211 Micro-Vickers hardness tester machine (Japan) was used to determine the fracture toughness by making imprints on the surface of the sample and measuring the length of the diagonals and cracks formed. In most cases, this method of monitoring can be regarded as being nondestructive (fracture surface area $\sim 0,01 \text{ mm}^2$). Investigations can be performed on samples of any shape and size. The accuracy of the method depends on the care taken in monitoring the condition of the surface, the measurement error of the dimensions of the microcracks, and the effect of the residual stresses. The attractiveness of the method based on the direct determination of the fracture toughness is due to the possibility of making repeated tests on small surface areas. The load can be chosen on the basis of the need to obtain microcracks of a definite type: relatively small loads – radial Palmqvist cracks (Fig. 2a), which as they grow transform into well-developed semi-disk-shaped median half-penny cracks (Fig. 2b).

To a significant degree, the characteristics of

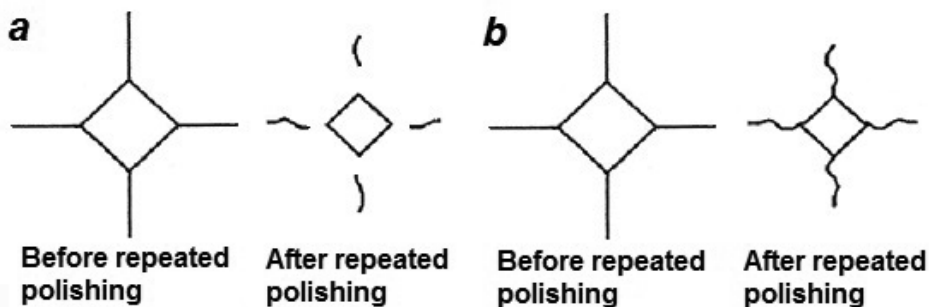


Figure 3. Palmqvist (a) and half-penny (b) cracks on the surface of a sample before and after repeated polishing

cracks become noticeable after the surface of the sample is repeatedly polished: in the case where Palmqvist cracks are formed, a region with undeformed material is formed around the imprint (Fig. 3). Therefore, a conclusion can be drawn about the characteristic form of the cracks arising under a given load.

The determination of the fracture toughness is based on the relation between the crack length L and the applied force P :

$$L = nP^{2/3}, \quad (3)$$

where n is the coefficient of proportionality [9].

The investigation of surface cracks [10] encompassed a wide range of elastic materials with fracture toughness $0,9\text{--}16 \text{ MPa}\cdot\text{m}^{1/2}$. The computational expression had the form

$$K_{1c} = \frac{0,15kH_V a^{1/2}}{\Phi} \left(\frac{c}{a}\right)^{-3/2}, \quad (4)$$

where $k \sim 3,2$ is a constant; $\Phi = H_V/\sigma_y \sim 3$ is a limiting factor; σ_y is the yield point, Pa; $a = (d_1 + d_2)/4$ is half the average length of the diagonal of the imprint, m; and c is the average length of a median crack, measured from the center of the imprint, m.

The following relation was obtained for median cracks [11]:

$$K_{1c} = 0,028H_V a^{1/2} \left(\frac{E}{H_V}\right)^{1/2} \left(\frac{c}{a}\right)^{-3/2}. \quad (5)$$

Subsequent investigations [12–14] showed that the initially formed cracks have the form of Palmqvist cracks. They propagate radially along the median planes and remain near the surface of the sample. Upon unloading, they grow in length and somewhat in depth. As the load increases, the formation of median cracks becomes the predominant character of fracture.

The relation (4) was transformed as follows on the basis of a large number of experimental results and a detailed mechanical and mathematical analysis:

$$K_{1c} = \frac{0,035H_V a^{1/2}}{\Phi} \left(\frac{E\Phi}{H_V}\right)^{2/5} \left(\frac{l}{a}\right)^{-1/2} \quad \text{- for Palmqvist cracks, (6)}$$

$$K_{1c} = \frac{0,129H_V a^{1/2}}{\Phi} \left(\frac{E\Phi}{H_V}\right)^{2/5} \left(\frac{c}{a}\right)^{-3/2}$$

- for half-penny cracks, (7)

where l is the average length of a Palmqvist crack, measured from the corner of the imprint, m [13, 14]. These expressions increased the reliability of the computed fracture toughness determined by the Vickers method. The results of the experiments using small (Palmqvist cracks) and large (median half-penny cracks) loads, calculated using relations (6) and (7), respectively, agree for materials whose elastic modulus lies in the range $43 \text{ GPa} \leq E \leq 407 \text{ GPa}$, the microhardness in the range $0,24 \text{ GPa} \leq HV \leq 72 \text{ GPa}$, the fracture toughness in the range

$0,5 \text{ MPa}\cdot\text{m}^{1/2} \leq K_{1c} \leq 13 \text{ MPa}\cdot\text{m}^{1/2}$ [12]. In the present work, these expressions were used to calculate the fracture toughness.

2. Results and Discussion

Young's modulus of a ceramic material can vary because of the presence of pores, dislocations, a second phase, and other microstructural defects. The effect of pores is especially large – the elastic modulus decreases with increasing porosity (decreasing density). The experimental Young's modulus of the fuel pellets correlates with the density $\sim 95\%$ TD (the theoretical density), as is generally accepted for uranium dioxide pellets [5] (Table 2). For almost equal density for pellets from all batches and therefore the same general porosity, the elastic modulus increases with increasing grain size, which, evidently, is associated with the differences in the number, shape, size, and spatial orientation of defects.

For small loads, there exists a region of high microhardness [3]. For this reason, it is necessary to determine the optimal load above which the microhardness remains almost constant, so that in some approximation it can be assumed to be independent of the applied force and suitable for a characteristic of the material.

To determine the optimal load of the experimental pellets, their microhardness was measured in the range $0,05\text{--}1 \text{ kg}$ in $0,05 \text{ kg}$ steps (Fig. 4). The loading time, duration of the testing force, and the unloading time were 7, 15, and 7 sec, respec-

Table 2. Mechanical properties of pellets

Batch	E , GPa	H_v , GPa	l/a_{av}	K_{1c} , $\text{MPa}\cdot\text{m}^{1/2}$
P1	184 (3)*	5,52 (0,04)	1,01	2,09 (0,04)
P2	197 (2)	5,73 (0,04)	2,19	1,46 (0,03)
P3	205 (2)	5,80 (0,04)	3,01	1,26 (0,03)

* The standard deviation is given in parenthesis.

tively, as the optimum for uranium dioxide [8]. A horizontal section of stabilization of the microhardness is observed for samples of all batches with load $\sim 0,5$ kg and average microhardness 5,5, 5,7, and 5,9 GPa for the batches P1, P2, and P3, respectively. Thus, subsequent measurements of the microhardness of the materials were performed under the load 0,6 kg (see Table 2). The imprints were made from the center along the radius in four mutually perpendicular directions on the surface of the sample. As a result, no dependence of the microhardness of the pellets on the coordinates of the imprint was found, which confirms the uniformity of the mechanical properties of the samples.

The microhardness of the pellets from batch P1 with grain size $13 \mu\text{m}$ is lower than that of the

pellets from batches P2 ($26 \mu\text{m}$) and P3 ($33 \mu\text{m}$), which corresponds to the theoretical notions concerning the reduction of the hardness of a polycrystalline material with decreasing size of its constituent crystallites [7, 8]. On the whole, the experimental microhardness of the pellets correlates with that of uranium dioxide [6–8].

The type of cracks arising on the surface of the experimental pellets was determined by comparing two series of photomicrographs of the imprints: before and after repeated polishing. In order for well-developed cracks to form, the force used to determine the fracture toughness of the materials is almost always greater than that used for measuring the microhardness. Thus, the load is 0,8–1 kg.

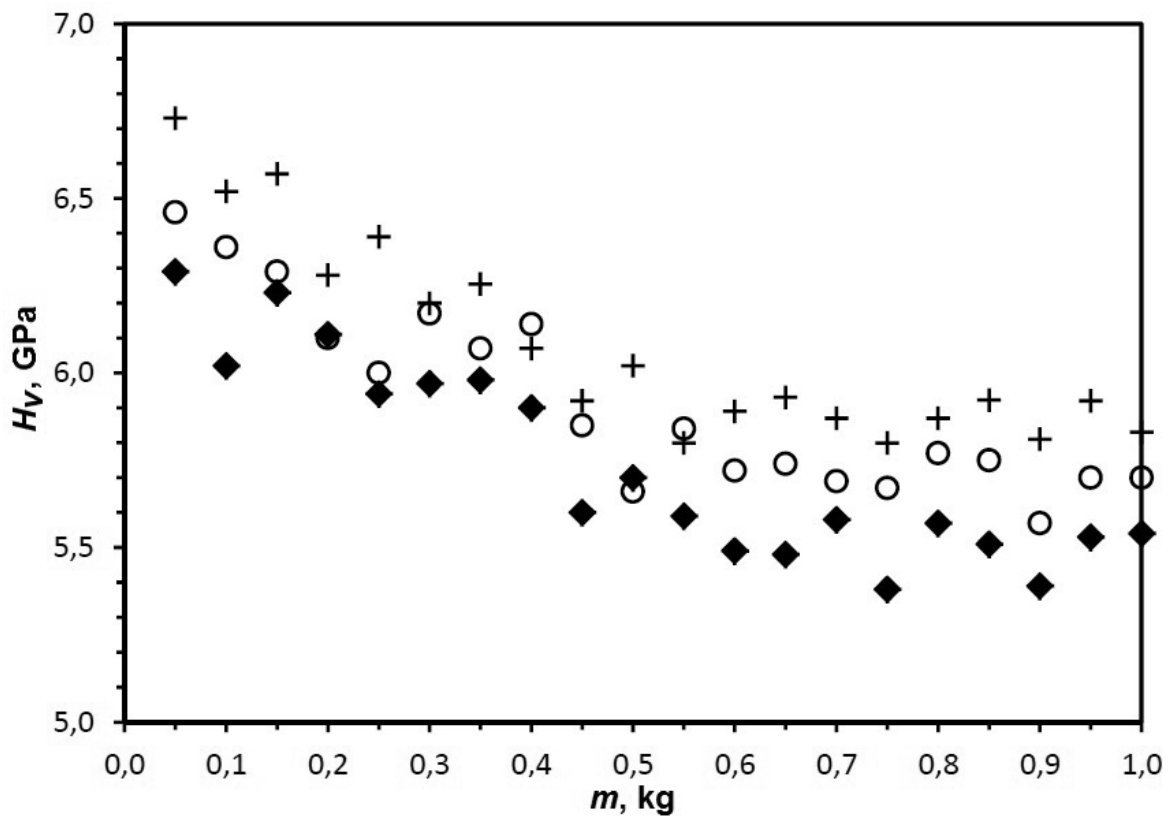


Figure 4. Microhardness versus the load for pellets from batches P1 (♦), P2 (○), and P3 (+)

It is evident in Figs. 5a, b that no visible changes are observed beneath the imprint in the experimental load range. Comparing Figs. 5c, d and Fig. 3a shows that the characteristic cracks formed in the experimental batches of pellets at loads up to 1 kg are Palmqvist cracks, which are characteristic of ceramic materials under relatively small loads.

To determine the fracture toughness, the pellets were subjected to loads up to 0,8 kg, since with larger forces asymmetric imprints with cleavages and a web of cracks were observed in some

cases. Imprints with the straightest Palmqvist cracks which were continuations of the diagonals of the imprints were used for measurements. Otherwise, strongly distorted results can be obtained.

The fracture toughness of pellets from batches with the smallest grains is higher than that of pellets from batches with large grains (see Table 2). This can be explained by the particularities of crack advancement in the samples. It is evident in Fig. 6 that for large grains (batch P3) the cracks propagate freely over a significant distance right

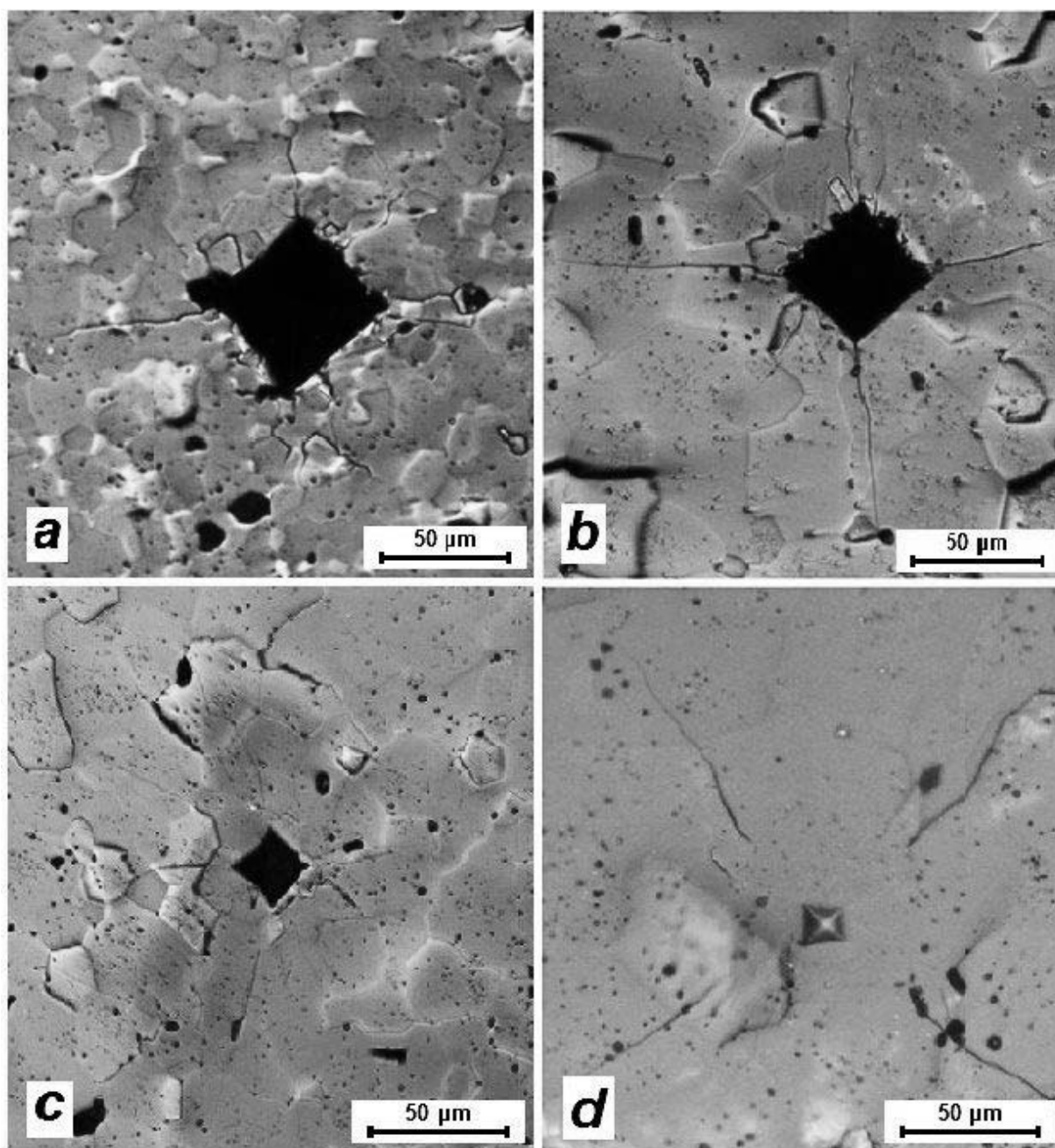


Figure 5. Characteristic appearance of the imprints and cracks on the surface of pellets from batches P1 and P2 after an imprint is made (a, b) and after repeated polishing (c, d)

through a grain (transgranular propagation); for smaller grains (batch P1) they propagate along grain boundaries with branching (intergranular propagation).

In small-grain materials, there exists a large resistance to intergranular propagation of cracks in the form of their blunting on large pores or a break in direction (reflection) of a crack on the grain boundaries [8]. Transgranular propagation is characteristic for materials with small pores and

large grains. In this case, a crack can propagate over distances several-fold longer than the diagonal of the imprint. On the whole there are three basic variants of crack propagation which are associated with the grain size and the porosity of the material [8] (Table 3). For the same load, the average length of the cracks formed on the surface of large-grain pellets is two–three times larger, which qualitatively confirms their lower fracture toughness (see Table 2 and Fig. 7).

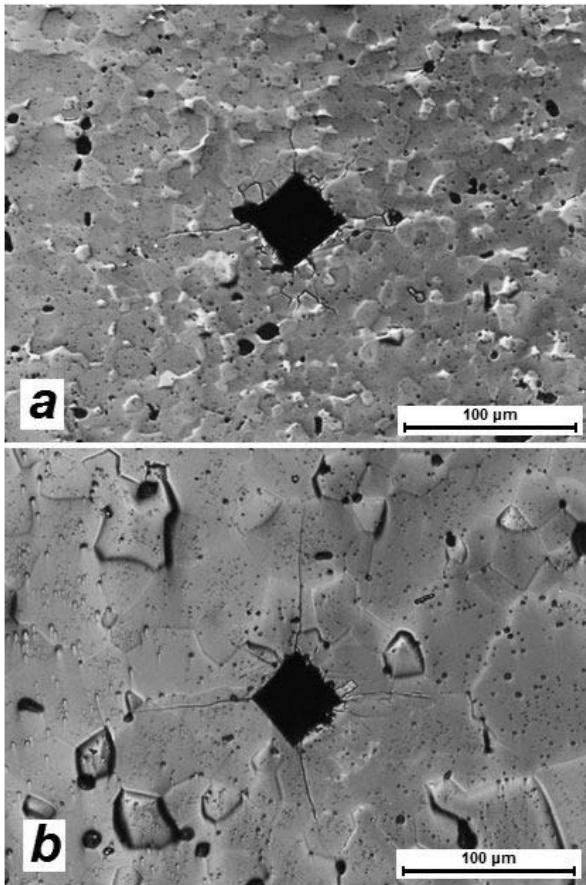


Figure 7. Cracks on the surface of pellets from batches P1 (a) and P2 (b)

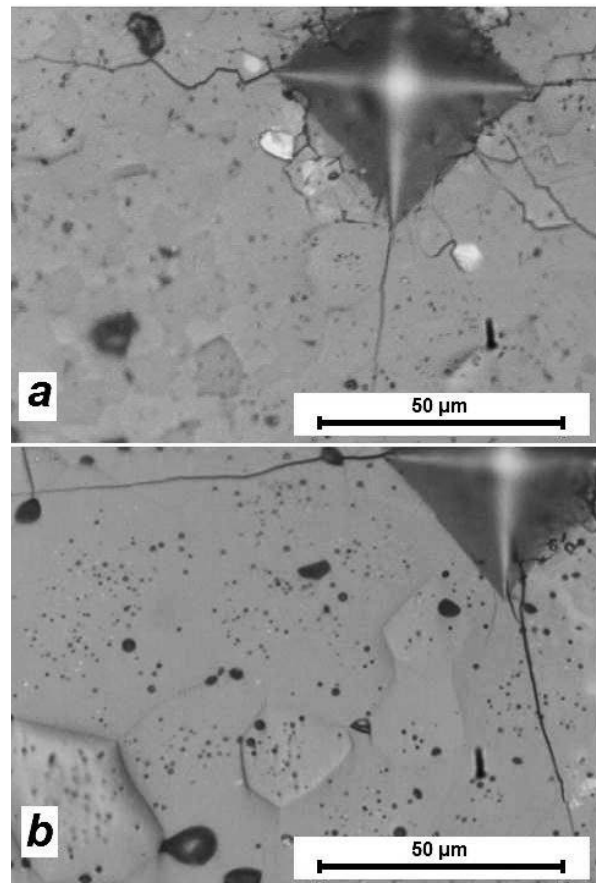


Figure 6. Cracks on the surface of pellets from batches P1 (a) and P3 (b)

Table 3. Crack propagation versus the microstructure of ceramic materials [8]

Case	Porosity type	Grain size	Type of crack propagation	Branching
1	Fine intergranular	Large	Transgranular	Not present
2	Large pores between grains	Small	Transgranular / Intergranular	Present
3	Channels from pores along grain boundaries	Small	Intergranular	Present

3. Conclusion

The investigation of crack formation in uranium oxide fuel pellets of the WWER-types showed that Young's modulus and the microhardness of polycrystalline samples increase with increasing grain size, while the fracture toughness decreases. Characteristically, radial Palmqvist cracks form on the surface of uranium dioxide pellets for loads up to 1 kg.

Transgranular propagation of cracks over distances several-fold larger than the length of the imprint diagonal is observed in pellets with large grains and small intragrain pores. Intergranular propagation of cracks along grain boundaries with branching occurs in pellets with small grains and low pore concentration on the grain boundaries. Blunting on large pores and at breaks in direction does not permit the cracks to reach a significant length.

References

- [1] G. Fantozzi, G. Orange, K. Liang, et al. Effect of nonstoichiometry of fracture toughness and hardness of yttrium glide ceramics. *J. Am. Ceram. Soc.*, 1989, v. 72, p. 1562 1563.
- [2] G.A. Gogotsi, S.N. Dub, E.E. Lomonova, B.I. Ozersky Vickers and Knoop indentation behaviour of cubic and partially stabilized zirconia crystals. *J. Europ. Ceram. Soc.*, 1995, v. 15, p. 405 413.
- [3] J. Gong, J. Wang, Z. Guan Indentation toughness of ceramics: A modified approach. *J. Mater. Sci.*, 2002, v. 37, p. 865 869.
- [4] H. Miyazaki, H. Hyuga, Y. Yoshizawa, et al. Relationship between fracture toughness determined by surface crack in flexure and fracture resistance measured by indentation fracture for silicon nitride ceramics with various microstructures. *Ceram. Intern.*, 2009, v. 35, p. 493 501.
- [5] A.R. Hall Elastic moduli and internal friction of some uranium ceramics. *J. Nucl. Mater.*, 1970, v. 37, p. 314 323.
- [6] K. Yamada, S. Yamanaka, M. Katsura Mechanical properties of (U,Ce)O₂. *J. Alloys Comp.*, 1998, v. 271 273, p. 697 701.
- [7] A.K. Sengupta, C.B. Basak, T. Jarvis, et al. Effect of titania addition on hot hardness of UO₂. *J. Nucl. Mater.*, 2004, v. 325, p. 141 147.
- [8] K. Kapoor, A. Ahmad, A. Lakshminarayana, G.V.S. Hemanth Rao Fracture properties of sintered UO₂ ceramic pellets with duplex microstructure. *Ibid.*, 2007, v. 366, p. 87 98.
- [9] B.R. Lawn, E.R. Fuller Equilibrium penny-like cracks in indentation fracture. *J. Mater. Sci.*, 1975, v. 10, p. 2016 2024.
- [10] A.G. Evans, E.A. Charles Fracture toughness determinations by indentation. *J. Am. Ceram. Soc.*, 1976, v. 59, p. 371 372.
- [11] B.R. Lawn, A.G. Evans, D.B. Marshall Elastic/plastic indentation damage in ce-ramics: The median/radial crack system. – *Ibid.*, 1980, v. 63, p. 574 581.
- [12] J. Lankford Indentation microfracture in the Palmqvist crack regime: implications for fracture toughness evaluation by the indentation method. *J. Mater. Sci. Lett.*, 1982, v. 1, p. 493 495.
- [13] K. Niihara, R. Morena, D.P.H. Hasselman Evaluation of K_{1c} of brittle solids by the indentation method with low crack-to-indent ratios. *Ibid.*, 1982, v. 1, p. 13 16.
- [14] K. Niihara A fracture mechanics analysis of indentation-induced Palmqvist crack in ceramics. – *Ibid.*, 1983, v. 2, p. 221 223.